RAPID COMMUNICATIONS

PHYSICAL REVIEW B VOLUME 52, NUMBER 18 1 NOVEMBER 1995-II

Static properties of the $S=1$ one-dimensional antiferromagnet $AgVP_2S_6$

M. Takigawa
IBM Thomas J. Watson Research Center, Yorktown Heights, New York 10598

T. Asano, Y. Ajiro, and M. Mekata
Department of Applied Physics, Fukui University, Fukui 910, Japan

(Received 17 July 1995)

NMR frequency shift has been measured at ^{51}V and ^{31}P sites in a single crystal of the one-dimensional spin-1 antiferromagnet $AgVP_2S_6$. Parameters in the single-ion spin Hamiltonian were determined from the orbital (van Vleck) shift at V sites. Temperature dependence of the spin shift (spin susceptibility) is consistent with the theoretical prediction and the magnitude of the Haldane gap determined from neutron-scattering experiments.

The existence of a spin excitation gap in spin-1 one-dimensional Heisenberg antiferromagnets first predicted by Haldane[1] is by now well established from experiments[2] and numerical calculations.[3,4] Although the excitation spectrum at $T=0$ is fairly well understood, we know relatively less about finite temperature properties. Recently, theories have been developed[5–7] for low-temperature static and dynamic properties based on a nonlinear σ model or a free boson (fermion) model. In this paper, we report the NMR frequency shift (K) at ^{51}V and ^{31}P nuclei in a single crystal of $AgVP_2P_6$, a spin-1 Haldane system. This material has a large excitation gap (26 meV) (Ref. 8) and is ideal for detailed study of low-temperature properties. We found that the temperature dependence of the spin susceptibility deduced from the shift data is consistent with the gap determined from neutron experiments and the theoretical prediction. We also determined parameters in the single-ion spin Hamiltonian from the anisotropic orbital shift. The spin dynamics based on the nuclear relaxation results will be discussed in a separate paper.

$AgVP_2S_6$ crystallizes in the monoclinic $P2/a$ structure[9] (Fig. 1). Each V^{3+} ion is surrounded by a distorted sulfur octahedron and has twofold point symmetry along the b axis. The V^{3+} ions form zigzag chains along the a axis. The magnetic susceptibility of the crystal used in the present experiments has been published earlier[10] and shows a low-temperature Curie tail corresponding to 0.3% $S=1/2$ impurity moments.

We first discuss the ^{51}V NMR spectra shown in Fig. 2(a), where the spin-echo intensity at 90 MHz is plotted against the magnetic field along various directions at 5 K. We observed equally spaced seven lines split by the electric quadrupolar interaction. The spacing between adjacent lines is given by $\Delta H=\{3eQ/\gamma_n\hbar 2I(2I-1)\}V_{zz}$ to the first order, where $I=7/2$ is the nuclear spin for ^{51}V, $\gamma_n=2\pi\times 11.193$ MHz/T the nuclear gyromagnetic ratio, Q the nuclear quadrupole moment, and $V_{zz}=\partial^2V/\partial z^2$ the zz component of the electric field gradient (EFG) tensor, where z is the magnetic field direction. The position of the center line is unaffected by the quadrupole interaction to first order but shifted by the magnetic hyperfine interaction between a nuclear spin (I) and electron orbital (L) and spin (S) moments,

$$\mathcal{H}_{\rm hf}=\hbar\gamma_n 2\mu_B\langle 1/r^3\rangle\sum_\alpha I_\alpha L_\alpha+\sum_{\alpha,\beta} I_\alpha A_{\alpha\beta}S_\beta, \qquad (1)$$

where $\langle 1/r^3\rangle$ is the expectation value of $1/r^3$ for $3d$ electrons and the spin hyperfine coupling tensor $A_{\alpha\beta}$ is to be determined from experiments. The magnetic shift is expressed as

$$K=K_{\rm orb}+K_{\rm spin},$$
$$K_{\rm orb}=2\langle 1/r^3\rangle\chi_{\rm orb}, \quad K_{\rm spin}=A\chi_{\rm spin}/(\hbar\gamma_n g\mu_B), \qquad (2)$$

where $\chi_{\rm orb}$ and $\chi_{\rm spin}$ is the orbital (van Vleck) and the spin susceptibilities. Since $\chi_{\rm spin}$ is negligibly small at low temperatures due to the large gap as we discuss later, $K_{\rm orb}$, which is independent of temperature, is equal to the measured K at 5 K.

We have determined the principal axes and values of $\nu_{\alpha\beta}=eQV_{\alpha\beta}/14h$ and $K_{\rm orb}$, as listed in Table I. From the crystal symmetry, the twofold b axis must be one of the principal axes of these tensors. The directions of other prin-

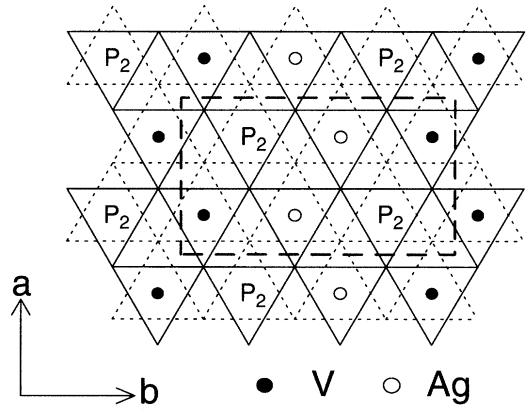

FIG. 1. Schematic structure of $AgVP_2S_6$ viewed from the c^* axis. V and Ag ions lie on the same plane. Sulfur network above (below) this plane is shown by the solid (dotted) lines. The dashed lines represent a unit cell. The angle between a and c axis is 106.6° (Ref. 9).

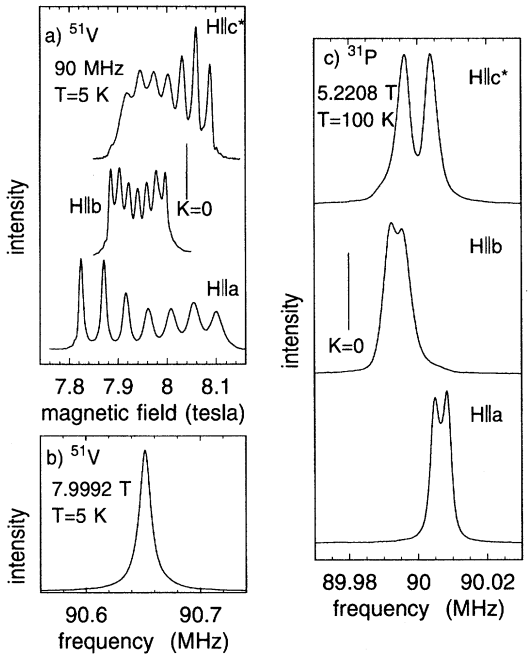

FIG. 2. NMR spin-echo spectra at ^{51}V sites (a), (b) and ^{31}P sites (c). The lines $K=0$ indicate the resonance in diamagnetic substances.

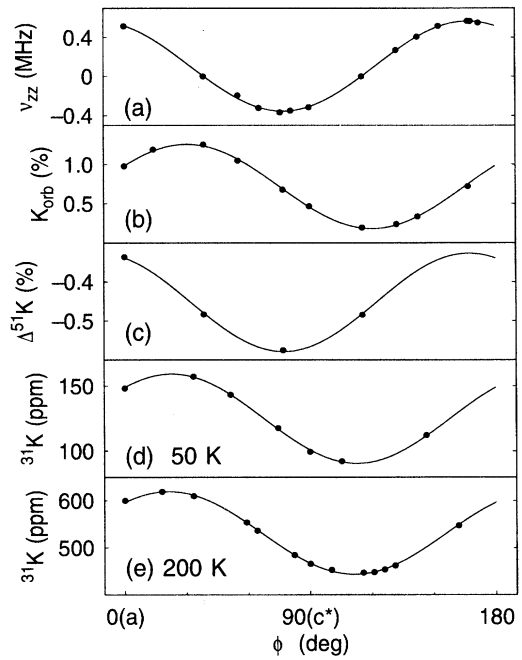

FIG. 3. Dependence of the zz component of various tensors on the magnetic field direction (z) rotated in the ac^* plane. (a) the quadrupole splitting at V sites, (b) the shift at V sites at 5 K (orbital shift), (c) the difference of the shift at V sites at 200 and 5 K, (d) the shift at P sites at 50 K, and (e) the shift at P sites at 200 K. The lines are fits to the form $A+B\cos^2(\phi-\theta)$.

cipal axes were determined from the dependences of ν_{zz} and $K_{\rm orb}$ on the magnetic field direction in the ac^*-plane as shown in Figs. 3(a) and 3(b). These principal axes are denoted as a' and c' in Table I (different for each quantity) and θ is the angle between a and a'. Corrections for higher order quadrupole effects were made in the evaluation of K. We observed two sets of quadrupole split lines for general field directions in the ac^* plane, indicating that the crystal has two domains of comparable volume. The results for only one domain are shown in Fig. 3. The data from the other domain are the mirror image of these with respect to the a or c^* axis, indicating that the two domains are related by 180° rotation around the a or c^* axis.

It is known that $\chi_{\rm orb}$ is related to the parameters in the single-ion spin Hamiltonian,

$$\mathcal{H}=\mu_B\sum_{\alpha,\beta}H_\alpha g_{\alpha\beta}S_\beta-\lambda^2\sum_{\alpha,\beta}S_\alpha\Lambda_{\alpha\beta}S_\beta, \qquad (3)$$

by the relations[11]

$$\Lambda_{\alpha\beta}=\frac{\chi_{{\rm orb},\alpha\beta}}{2\mu_B^2}=\sum_n\frac{\langle 0|L_\alpha|n\rangle\langle n|L_\beta|0\rangle}{E_n-E_0},$$

$$g_{\alpha\beta}=2(\delta_{\alpha\beta}-\lambda\Lambda_{\alpha\beta}), \qquad (4)$$

where λ is the spin-orbit coupling. These parameters can be determined from $K_{\rm orb}$ by using the free ion values $\langle 1/r^3\rangle=3.22$ a.u. and $\lambda=104$ cm^{-1}.[11] The estimated g value is given in Table I. The anisotropy energy is usually expressed as $DS_\zeta^2+E(S_\xi^2-S_\eta^2)$, where $D=-\lambda^2[\Lambda_{\zeta\zeta}-(\Lambda_{\xi\xi}+\Lambda_{\eta\eta})/2]$ and $E=-\lambda^2(\Lambda_{\xi\xi}-\Lambda_{\eta\eta})$ with ξ, η, and ζ being the a', b, and c' directions for $K_{\rm orb}$. We then obtain

$$D=4.5\ \text{K}, \quad |E|\leq 0.1\ \text{K}, \qquad (5)$$

TABLE I. Principal values of EFG, orbital shift, g values, and spin hyperfine coupling tensors at ^{51}V and ^{31}P sites. The b axis is a principal axis for all quantities. Other principal axes in the ac^* plane are denoted by a' and c' and θ is the angle between a and a'.

	b	a'	c''	θ (deg)
$\nu_{\alpha\alpha}$ (MHz)	−0.21±0.01	0.57±0.01	−0.36±0.01	−13±2
$K_{\rm orb}$ (%)	1.25±0.01	1.25±0.01	0.17±0.01	31±2
g	1.931	1.931	1.990	
$A/\hbar\gamma_n$ (V) (T)	−28.6±0.5	−15.5±0.7	−27.4±0.5	−14±4
$A/\hbar\gamma_n$ (P) (T)	2.01±0.02	2.17±0.02	1.62±0.02	21±2
	2.01±0.02	2.14±0.02	1.65±0.02	−17±2

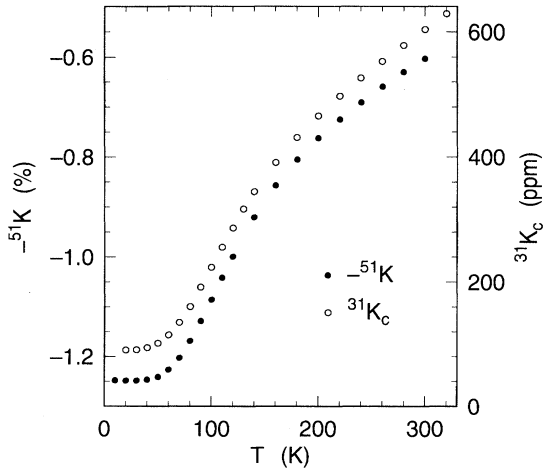

FIG. 4. Temperature dependence of the shifts at ^{51}V sites along the magic angle (solid circles; note the negative sign) and at ^{31}P sites along the c^* axis (open circles).

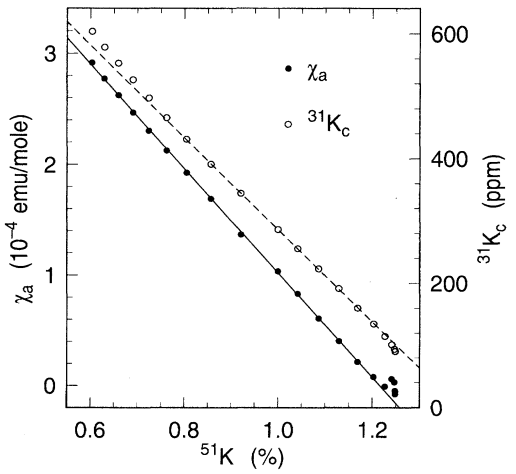

FIG. 5. The corrected magnetic susceptibility along the a axis (χ_a; solid circles) and the shift at P sites along the c^* axis ($^{31}K_c$; open circles) are plotted against the shift at V sites along the magic angle (^{51}K).

indicating the nearly uniaxial easy-plane type anisotropy. The value of D is more than an order of magnitude larger than the previous estimation[12] based on an empirical analysis of the susceptibility anisotropy. Uncertainty in our estimate of D is mostly due to covalent bonding effects that may change $\langle 1/r^3 \rangle$ and λ from the free ion values but will be at most about 20%.[13]

Since EFG is a traceless tensor, there is a line of directions (magic angles) along which $\nu_{zz}=0$, yielding a single resonance line. The Fourier-transformed (FT) spin-echo spectrum in Fig. 2(b) is obtained along such a magic angle lying in the ac^* plane. The sharp resonance line enabled accurate determination of K (typical accuracy of 10 ppm). The temperature dependence of K thus determined is shown in Fig. 4 by solid circles. Unlike the bulk susceptibility, which shows a Curie-Weiss tail due to impurities, K becomes completely flat at low temperatures and provides accurate temperature dependence of the intrinsic spin susceptibility. Shimizu *et al.* have recently measured the shift at Y sites in another Haldane system Y_2BaNiO_5 and obtained a similar temperature dependence.[14]

We next turn to the results on ^{31}P sites. The FT spin-echo spectra at ^{31}P sites are shown in Fig. 2(c). A ^{31}P nucleus has spin 1/2 and hence no quadrupole moment. Since two P atoms in the unit cell are closely located, the spectra show two peaks split by the nuclear dipolar interaction. The shift is determined from the average position of the two peaks. (All P sites in the unit cell are equivalent.) The temperature dependence of K at P sites along the c^* direction ($^{31}K_c$) is shown in Fig. 4 by open circles.

Let us now discuss the spin hyperfine coupling at both sites. In Fig. 5, the shift at V sites along the magic angle (^{51}K) is plotted against χ_a (bulk susceptibility along the a direction corrected for the impurity Curie-Weiss term), showing a good linear relation (solid circles). From this plot and Eq. (2), we obtain $A_{zz}/(\hbar\gamma_n)=-23.2$ T for this direction. (We have used the estimated anisotropy of g.) Then we measured the orientation dependence of the difference of ^{51}K at 200 and 5 K as shown in Fig. 3(c), from which the principal axes and values of the hyperfine coupling tensor A were determined and given in Table I. The isotropic part of $A/(\hbar\gamma_n)$ is -23.8 T, a typical value for the core polarization field.

We made a similar analysis for the shift at P sites. The open circles in Fig. 5 show the plot of $^{31}K_c$ vs ^{51}K. Both shifts are in a good linear relation at low temperatures but deviate from the linearity at high temperatures (above 200 K). This indicates slight increase in the hyperfine coupling at P sites at high temperatures, which could be due to small shift of the position of P atoms in the unit cell. The principal axes and values of A at P sites at low temperatures were determined from the orientation dependence of the difference of K at 50 K [Fig. 3(d)] and 200 K [Fig. 3(e)]. These are given in the lower part of Table I. Since $A \propto K_{\rm spin} g/\chi_{\rm spin} \propto K_{\rm spin}/g$ [Eq. (2)] and the anisotropy of g was determined from the shift at V sites, the presence of two domains in our crystal mentioned before leads to two possible sets of A at P sites as shown in the table, corresponding to the different angles between the principal axes of g and $K_{\rm spin}$. The two results, however, are not much different. The hyperfine coupling at P sites is large and dominantly isotropic, indicating the significant hybridization between P and V orbitals.

Finally we compare the temperature dependence of $\chi_{\rm spin}$ obtained from the shift data with theoretical calculation. Jolicoeur and Golinelli[7] have calculated the spin susceptibility in the Haldane system using a nonlinear σ model, which reduces to the result of a free boson model in the low-temperature limit obtained earlier by Affleck.[5] In a free boson model, the magnon dispersion relation near the wave vector π,

$$\varepsilon=\sqrt{v^2(k-\pi)^2+\Delta^2}, \tag{6}$$

leads to

$$\chi_{\rm spin}=\frac{2(g\mu_B)^2}{v\sqrt{2\pi}}\sqrt{\frac{\Delta}{T}}\exp(-\Delta/T), \tag{7}$$

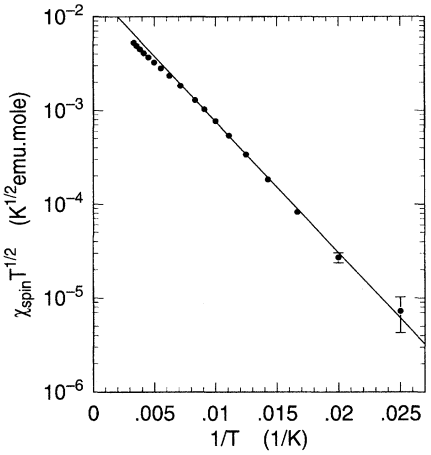

FIG. 6. The spin susceptibility multiplied by $\sqrt{T}$ is plotted against $1/T$.

where we have neglected the effects of small anisotropy and the field dependence of the gap.[15] In Fig. 6, $\chi_{\rm spin}\sqrt{T}$ is plotted against $1/T$, where $\chi_{\rm spin}$ is determined from the ^{51}K data in Fig. 4 after subtracting the constant orbital shift. The data can be fit to $\chi_{\rm spin}\sqrt{T}=C\exp(-\Delta/T)$ with $\Delta=320$ K (27.5 meV) and $C=1.90\times10^{-2}$ $K^{1/2}$ emu/mole, in agreement with Eq. (7). The value of Δ is in good agreement with the neutron-scattering experiment on polycrystalline sample ($\Delta=26$ meV).[8] In addition, from the results of numerical simulation ($\Delta=0.41$ J, $v=2.49$ J),[16] the prefactor in Eq. (7) is calculated as $2(g\mu_B)^2\sqrt{\Delta}/(v\sqrt{2\pi})=1.04\times10^{-2}$ $K^{1/2}$ emu/mole, which is not very far from the value of C. Thus a free boson model appears to give an adequate account of the spin susceptibility. The value of the gap combined with the anisotropy [Eq. (5)] gives the ratio $D/J=5.8\times10^{-3}$, which is much smaller than other Haldane antiferromagnets such as NENP and Y_2BaNiO_5.

The effect of anisotropy DS_ζ^2 on the spin susceptibility has been studied theoretically.[5] First, the gap now depends on the polarization direction of the excited magnon. According to the numerical calculation,[17] the splitting of the gap $\Delta_\zeta-\Delta_\xi$ is about 1.8 D, which is much smaller than the average gap in our case. Second, the spin susceptibility in the $\xi\eta$ plane is not zero at $T=0$. Its upper limit is estimated as[5] $\chi_{{\rm spin},\xi}(T=0)<(g\mu_B)^2(\Delta_\zeta-\Delta_\xi)^2/2\Delta^3$ and the corresponding spin shift at V sites should be smaller than 2.7×10^{-5}, which is negligible compared with the observed anisotropy of K at 5 K ($\sim1\%$). This justifies our initial assumption that the spin shift is zero at low temperatures.

In conclusion, we have determined the single-ion anisotropy and the hyperfine coupling tensors at V and P sites in $AgVP_2S_6$ from the NMR shift measurements. The temperature dependence of the spin susceptibility is consistent with the theoretical prediction and gives the value of the gap which agrees with the neutron-scattering results.

We are grateful to E. T. Ahrens for technical assistance and I. Affleck for helpful discussions.

[1] F. Haldane, Phys. Lett. **93A**, 464 (1983).
[2] J. Renard *et al.*, Europhys. Lett. **3**, 945 (1987).
[3] M. Nightingale and H. Blote, Phys. Rev. B **33**, 659 (1986).
[4] M. Takahashi, Phys. Rev. Lett. **62**, 2313 (1989).
[5] I. Affleck, Phys. Rev. B **41**, 6697 (1990).
[6] A. M. Tsvelik, Phys. Rev. B **42**, 10 499 (1990).
[7] T. Jolicoeur and O. Golinelli, Phys. Rev. B **50**, 9265 (1994).
[8] H. Mutka *et al.*, Phys. Rev. Lett. **67**, 497 (1991).
[9] S. Lee, P. Colombet, G. Oucrard, and R. Brec, Mater. Res. Bull. **21**, 917 (1986).
[10] T. Asano *et al.*, Solid State Commun. **88**, 795 (1994).
[11] A. Abragam and B. Bleaney, *Electron Paramagnetic Resonance of Transition Ions* (Clarendon, Oxford, 1970).
[12] C. Payen, P. Molinie, P. Colombet, and G. Fillion, J. Magn. Magn. Mater. **84**, 95 (1990).
[13] J. Owen and J. H. M. Thornley, Rep. Prog. Phys. **29**, 675 (1966).
[14] T. Shimizu, D. E. MacLaughlin, P. C. Hammel, J. D. Thompson, and S. W. Cheong (unpublished).
[15] Eq. (2.14) in Ref. 5 has an error. The correct expression is given here [I. Affleck (private communication)].
[16] E. Sorenson and I. Affleck, Phys. Rev. Lett. **71**, 1633 (1993).
[17] T. Sakai and M. Takahashi, Phys. Rev. B **42**, 4537 (1990).